Heliyon 10 (2024) e24940

Contents lists available at ScienceDirect

Heliyon

journal homepage: www.cell.com/heliyon

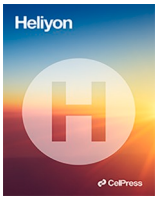

Research article

Towards long-term operation of flow-electrode capacitive deionization (FCDI): Optimization of operating parameters and regeneration of flow-electrode

Wanni Zhang [a], Wenchao Xue [a,*], Chunpeng Zhang [b,**], Kang Xiao [c]

[a] Department of Energy, Environment and Climate Change, School of Environment, Resources and Development, Asian Institute of Technology, P.O. Box 4, Klong Luang, Pathumthani, 12120, Thailand

[b] Key Laboratory of Groundwater Resources and Environment (Ministry of Education), College of New Energy and Environment, Jilin University, Changchun, 130021, China

[c] College of Resources and Environment, University of Chinese Academy of Sciences, Beijing, 100049, China

ARTICLE INFO

Keywords:
Flow-electrode capacitive deionization (FCDI)
Operating parameters
Sensitivity analysis
Electrode regeneration
Long-term operation

ABSTRACT

This study systematically optimized the key operating parameters and interpreted their effecting mechanisms in a flow-electrode capacitive deionization (FCDI) system. The optimal voltage, activated carbon electrode content, electrolyte concentration, feedwater flowrate, and electrode flowrate for desalinating low salinity feedwater (1.0 g L^{-1} NaCl) were determined to be 1.8 V, 2.0 wt%, 10.0 g L^{-1}, 80 mL min^{-1}, and 60 mL min^{-1}, respectively. The variations of the above parameters can affect the system conductivity, the thickness and stability of the electric double layers, and/or the degree of concentration polarization, thereby influencing the desalination performance. Moreover, a sensitivity analysis identified the operating voltage as the dominant parameter with the most significant influence on the FCDI system. Subsequently, a long-term operation was carried out under single-pass mode. The results showed that the lab-scale FCDI system was able to constantly maintain the desalination efficiency of 1.0 g L^{-1} feedwater (NaCl) at 40–60 % for multiple operating cycles. Over 99.8 % of electrode material regeneration and desalination efficiency recovery was able to be obtained during a 60-h operation, demonstrating that the FCDI system showed strong stability and long-term operation potential.

1. Introduction

In recent decades, the rising demand brought about by human development and the continuous consumption of limited freshwater resources has become one of the key contradictions affecting sustainable development. Especially in coastal areas, seawater intrusion intensified by climate change makes freshwater a scarce resource. To alleviate such pressure, the development and application of desalination technology are essential. At present, a variety of desalination technologies with different mechanisms are in full bloom, and the most common mature technologies include RO (reverse osmosis), ED (electrodialysis), MSF (multi-stage flash distillation), MED (multi-effect desalination), etc [1–4]. These commercialized technologies possess the advantages of high desalination efficiency and stable performance; however, their shortcomings cannot be ignored. RO and MSF/MED require high pressure/temperature while

* Corresponding author.
** Corresponding author.
E-mail addresses: wenchao@ait.ac.th (W. Xue), zhang_cp@jlu.edu.cn (C. Zhang).

https://doi.org/10.1016/j.heliyon.2024.e24940
Received 18 September 2023; Received in revised form 11 January 2024; Accepted 17 January 2024
Available online 20 January 2024
2405-8440/© 2024 Published by Elsevier Ltd. This is an open access article under the CC BY-NC-ND license (http://creativecommons.org/licenses/by-nc-nd/4.0/).

operating, hence greenhouse gases are produced from energy supply equipment (e.g., MSF produces about 30 g NO_x per cubic meter of water processed). Whereas ED has the disadvantage of high-level energy costs due to its high operating voltage [1].

In response, capacitive deionization (CDI) has gradually developed in recent years as an emerging desalination technology via a low-voltage electrosorption process. Compared with the abovementioned conventional desalination technologies, CDI has the advantages of low energy consumption, low emission, and high desalination efficiency [5–7]. To further optimize the adsorption capacity, Jeon et al. [8] developed flow-electrode capacitive deionization (FCDI) by replacing solid electrodes in CDI with flow-electrodes. Thus, flow-electrodes enabled a continuous adsorption/desorption process in FCDI systems.

FCDI has received extensive attention since its inception. Studies on it can be divided into the following areas in descending order of number: process development, electrode optimization, mechanistic studies, and cell construction [9,10]. In 2013, the first FCDI reactor with a three-chamber 2D structure was designed by Jeon et al. [8]. Gendel et al. created a continuous system utilizing two FCDI cells. In terms of electrodes based on carbon materials such as activated carbon, related studies have been made on optimization by various means [11]. For instance, functional groups such as carboxyl were introduced by chemical oxidation to enhance the carbon loading [12]; charge-transfer materials (e.g., $NaMnO_2$) with high ion capture capacity were applied [13]; nano-additives such as carbon nanotubes and superconducting carbon black played the roles of charge paths [14–16].

In terms of mechanism research, Nativ et al. reported on the desalination mechanism and Faradaic reaction by observing the state and products of the flow-electrode, while Rommerskirchen et al. conducted a modeling study on the process of FCDI desalination [17,18]. Furthermore, the configuration of FCDI cells is also one of the research hot spots. Cho et al. designed a multi-channel FCDI cell with a 3D structure which greatly increased the desalination rate, while Ma et al. optimized the FCDI cell by employing membrane stacking [19,20]. In addition to focusing on desalination, FCDI has gradually appeared in resource recovery, energy recovery, and other fields [21,22]. However, most previous studies focused on unilateral optimization without aiming at systematic operating parameter evaluation. Moreover, long-term operations on FCDI are still rare. Ma et al. performed an 11-h long-term test using the activated carbon/carbon black flow-electrode [23]. Yet, the test ran for only a short time. Hence, it did not reflect the reusability of electrode materials or the system stability.

This study systematically investigated the effects of five crucial parameters on the desalination rate and energy efficiency of FCDIs, including operating voltage, activated carbon (AC) electrode content, electrolyte concentration, feedwater flowrate, and electrode flowrate. These key operating parameters may potentially affect the performance of an FCDI with the following considerations: 1) the operating voltage may influence the moving rate of ions and the thickness of the electrical double layers (EDLs) on the surface of the electrode materials [15]; 2) the content of AC may affect the conductivity and adsorption capacity of the flow-electrode [24]; 3) the electrolyte concentration may simultaneously affect the conductivity of flow-electrode and the concentration gradient of ions across the ion exchange membranes; 4) the feedwater flowrate may affect the concentration polarization (CP) of the FCDI system [25,26]; and 5) the electrode flowrate may impact on the adsorption of ions by affecting the stability of EDLs [27].

To identify the dominant parameters, sensitivity analysis was employed. Furthermore, a multi-cycle long-term operation with flow-electrode regeneration and recovery was carried out to investigate the feasibility and stability of FCDI.

2. Materials and methods

2.1. Flow-electrode preparation

Analytical grade activated carbon (AC, Sinopharm Group, China) powder possessing a particle size ranging between 10–50 μm was used as the flow-electrode material in this study. To improve the suspension and dispersion of AC power in the flow-electrode during operation, a low dosage of sodium dodecyl sulfate (SDS) purchased from Sigma Aldrich (USA) was applied as the dispersant. Synthetic feedwater and electrolyte were prepared using analytic grade NaCl (Sinopharm, China).

The flow-electrode slurry was prepared by mixing the AC powder at a designed weight proportion into 100 mL of NaCl electrolyte (see Table 1). A constant dosage of SDS at 0.1 g L^{-1} was used in all flow-electrodes with varied AC contents and electrolyte concentrations. The flow-electrode slurries were mixed using an ultrasonic diffuser (GT–SONIC–D27, GT Ultrasonic, China) prior to any batch experiment. SDS can promote the stable dispersion of activated carbon in electrolytes [28]. Cai et al.'s study stated that adding SDS effectively improved the desalination performance of FCDI [29]. In addition, due to the selective permeability of the ion exchange membrane, it was expected that the SDS in the flowing electrode would not be released into the water chamber. In addition, a magnetic stirrer (MR Hei-Mix S, Heidolph, Germany) continuously blended the electrode slurry at a low speed to ensure the homogeneity of the flow-electrode during the operation.

Table 1
Design of selected operating parameters in the batch FCDI for performance optimization.

Parameters	Unit	Examined values						
Voltage	V	0.8	1.0	1.2	1.4	1.6[a]	1.8	2.0
AC content	wt. %	0.5	1.0	1.5	**2.0**[a]	3.0	5.0	7.0
Electrolyte concentration	g L^{-1}	1.0	2.5	5.0	**7.5**[a]	10.0	12.5	15.0
Feedwater flowrate	mL min^{-1}	10	20	40	**60**[a]	80	100	120
Electrode flowrate	mL min^{-1}	60		80	**100**[a]	120		140

[a] Initial setting of FCDI operating parameters in the batch tests.

2.2. Laboratory-scale FCDI reactor setup

A lab-scale FCDI system was designed and assembled as shown in Fig. S1. Owing to the effective dimensions of 130 × 130 × 40 mm, the FCDI cell was composed of two acrylic end plates, two stainless steel current collectors, one piece of anion exchange membrane (AEM, HMTECH-1680T, Huamotech Co., Ltd., China), one piece of cation exchange membrane (CEM, HMTECH-1680T, Huamotech Co., Ltd., China), and one feedwater chamber. The stainless steel plates were engraved with serpentine channels (2 mm in depth and 3 mm in width), aiming at enlarging the contact area between current collectors and flow-electrodes, hence ensuring a uniform and stable charge distribution [9]. The ion exchange membranes with selective permeation of anions or cations prevented the electrode slurry from spillage and simultaneously avoided the negative influence caused by the co-ion effect [30]. A 3-mm wide feedwater channel was designed in between the ion exchange membranes.

The FCDI system was empowered by a low-voltage DC power supply (GPS305D-30V5A, Wanptek, China). The flow-electrode slurry was supplied by a peristaltic pump (Masterflex, USA) to the flow-electrode channels inside the current collectors and circulated in a short-circuit closed-cycle (SCC) mode. The SCC mode is a typical FCDI mode of operation that allows the cathode and anode to be electrically neutralized as they flow back into the electrode reservoir, thereby completing the automatic desorption of ions [21]. This made the adsorption capacity of the electrode material no longer the main factor limiting FCDI.

2.3. Batch mode operation

The effects of concerned operating parameters, namely, operating voltage, AC content, electrolyte concentration, feedwater flowrate, and electrode flowrate in FCDI and their optimized combinations were explored using the orthogonal experimental design method. According to previous literature [15,20,24,31], the initial setting of the abovementioned parameters was designed at an operating voltage of 1.6 V, AC content of 2.0 wt%, electrolyte concentration of 7.5 g L^{-1}, feedwater flowrate of 60 mL min^{-1}, and electrode flowrate of 100 mL min^{-1} for both anode and cathode sides, respectively. These parameters were then varied individually with the others remaining unchanged, as described in Table 1, to optimize the desalination performance in the FCDI. For all batch tests, a feedwater containing 100 mL of 1 g L^{-1} NaCl was circulated in the feed channel, and the variation in conductivity (EC) of the feedwater was monitored over a duration of 120 min.

Sensitivity analyses of selected operating parameters to the performance of FCDI were done using spider plots [32]. The sensitivity was evaluated between −50 % and +50 % for the initial operating voltage, AC content, electrolyte concentration, feedwater flowrate, and electrode flowrate. The variations in Average Salt Adsorption Rate (ASAR) and Energy-normalized Removed Salt (ENRS) were regarded as indicators. The gradients of the lines indicated the degree of sensitivity. The steeper the curve, the more sensitive the ASAR/ENRS was to the corresponding parameter.

2.4. Long-term operation of the FCDI system

The lab-scale FCDI system was operated for a total of 170 h, including three repetition cycles. A total volume of 8 L feedwater containing 1 g L^{-1} NaCl was fed into the FCDI reactor with the operation mode switched from batch mode to single-pass mode. In single-pass mode, there was only one chance for the feedwater to pass through the water chamber, hence the hydraulic retention time was extended by reducing the flowrate. The feedwater flowrate was adapted to 1–4 mL min^{-1} to ensure an acceptable desalination rate, whereas the other parameters were determined based on the optimization in sections 2.2 and 2.3. After each operating cycle, the desalination process was temporarily interrupted, and the electrode material (AC) in the electrode slurry was recovered and regenerated for the next cycle.

The regeneration of flow-electrode material was performed using a microfiltration process. Three alternative filter membranes, namely PTFE Membrane Filter (47 mm, 0.45 μm, from Vertical Chromatography Co., Ltd., Thailand), NYL Membrane Filter (50 mm, 0.45 μm, from Vertical Chromatography Co., Ltd., Thailand), and Cellulose Acetate Filter (47 mm, 0.2 μm, from Sartorius Stedim Biotech, Germany) were tested using a laboratory vacuum filtration system. The flow-electrode retained by filter membranes were then re-dispersed and recovered through three procedures, i.e., soaking in the electrolyte solution for 30 min, ultrasonic cleaning for 10 min + soaking for 20 min, and ultrasonic cleaning for 30 min. Each cleaning scheme consumed 100 mL of distilled water to rinse the membrane. The percentage recovery of flow-electrode was weighted and compared among the abovementioned procedures, and the recovery method with the highest recovery rate was selected as the regeneration scheme for the long-term operation of FCDI.

2.5. Laboratory and data analysis

A conductivity meter (Seven2Go™ Conductivity Meter-S3, Mettler Toledo, Switzerland) was applied to measure the EC of the feedwater, and the NaCl concentration was determined from the linear correlation between the EC and the NaCl concentration (see Fig. S2 for the calibration curve). The operating voltage (V) and current (I) of the DC power supply were monitored.

Maximum salt adsorption rate (SAR_{max}, $\mu g \cdot cm^{-2} \cdot s^{-1}$) and average salt adsorption rate (ASAR, $\mu g \cdot cm^{-2} \cdot s^{-1}$) are calculated based on the variation in NaCl concentration of feedwater, which measures the maximum salt adsorption rate and average salt adsorption rate of FCDI, respectively. In batch mode, the desalination rate continuously decreased with the decline of feedwater concentration. Therefore, the first two sets of data recorded by the conductivity meter (i.e., 0 and 5 min) were utilized to calculate SAR_{max}. The two parameters are determined in eq. (1) and eq. (2):

$$SAR_{max} = \frac{(C_0 - C_5) \times V_f}{A \times 5mins} \quad (1)$$

$$ASAR = \frac{(C_0 - C_t) \times V_f}{At} \quad (2)$$

where C_0 and C_t are the NaCl concentrations (mg·L^{-1}) at time 0 and t, respectively; V_f is the volume of the feedwater, L; A is the effective contact area between the ion exchange membrane and the flow-electrode, cm^2.

Charge efficiency refers to the utilization rate of the input charge by the flow-electrode, which is expressed by the ratio of the charge consumption in the electrosorption desalination process to the total charge supplied [33]. It is determined in eq. 3

$$\Lambda = \frac{N_A e \frac{(C_0 - C_t) \times V_f}{M}}{\int Idt} \times 100\% \quad (3)$$

where, e is the elementary charge, C; N_A is the Avogadro constant, mol^{-1}; M is the molar mass of desalinated NaCl, 58.5 g mol^{-1}; and I is the current input measured in A.

Energy-normalized removed salt (ENRS, μmol·J^{-1}) reflects the amount of salt being removed by per unit of energy. It is determined in eq. (4).

$$ENRS = \frac{V_f(C_0 - C_t)}{V \int Idt} \quad (4)$$

3. Results and discussion

3.1. Factors affecting the performance of FCDI

3.1.1. Effect of operating voltage

The effect of the operating voltage provided to the electrodes of FCDI was examined at a relatively low voltage range (i.e., 0.8–2.0 V) compared to several previous reports (i.e., 0.6–4.8 V) [20,34,35]. This voltage range included the commonly applied voltage on capacitive deionization systems (0.8–1.2V) and the voltage slightly higher than the critical limit of water electrolysis (1.23–2.0V) [36]. The determination of such a voltage range took into account both the diversity of voltage stages and the demand for low energy consumption. Although slight electrolysis occurred at a voltage of above 1.23V, according to the current-voltage curve obtained from previous studies, the impact of electrolysis at low voltages (0.8~2V) on the conductivity of the FCDI system was possible to be negligible [37]. The other operating parameters were set at the initial values as described in Section 2.3. The desalination performance represented by SAR_{max} and ASAR and energy efficiency, represented by charge efficiency and ENRS in the lab-scale FCDI under different operating voltages, are presented in Fig. 1A. Meanwhile, the potential mechanism is illustrated in Fig. 1B.

It was observed that the SAR_{max} of FCDI raised continuously from 0.22 ± 0.01 μg cm^{-2} s^{-1} up to 0.90 ± 0.02 μg cm^{-2} s^{-1} as the voltage increased from 0.8 to 2.0 V. A similar trend of ASAR increment from 0.13 ± 0.01 μg cm^{-2} s^{-1} at 0.8 V to 0.35 ± 0.02 μg cm^{-2} s^{-1} at 2.0 V was observed. This observation is supported by a previous study on FCDI fed with a flow-electrode composed of 30 g L^{-1} Na_2SO_4 and 1.0 wt% CB, in which the desalination rate increased from 0.52 μg cm^{-2} s^{-1} to 4.08 μg cm^{-2} s^{-1} with the operating voltage increasing from 0.6 V to 4.8 V [15]. Notably, both SAR_{max} and ASAR increased non-linearly, with a greater acceleration as the voltage raised. This was possibly due to the combined effect of the elevated electric field strength in the cell and the accumulated free charges

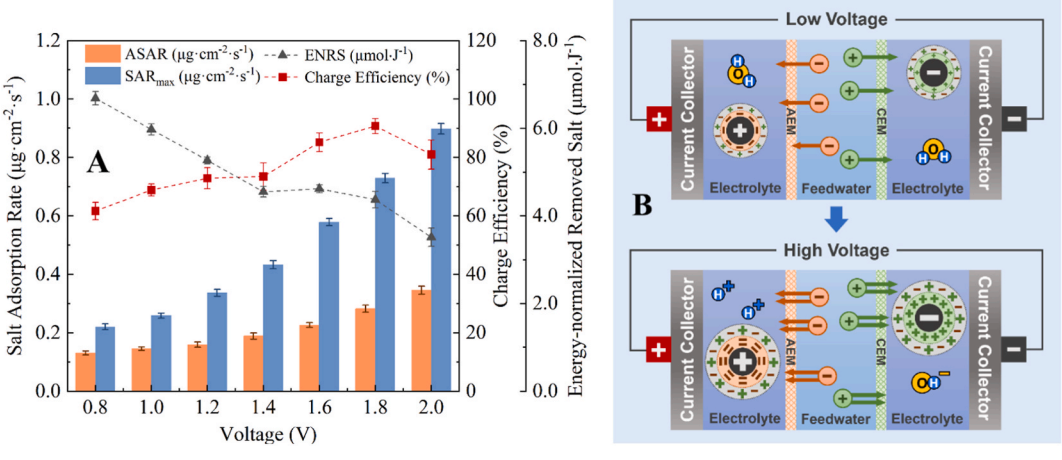

Fig. 1. Desalination performance analysis (A) and mechanism diagram (B) of FCDI system at different voltages.

in the EDLs surrounding the flow-electrodes as the operating voltage increased in FCDI. The former enhanced the driving force for deionization and hence accelerated the migration of ions between the electrodes, while the latter increased the thickness of EDLs and hence advanced the counter-ion adsorption capacity of flow-electrodes [38].

The energy efficiency of FCDI was assessed using multiple variables, i.e., ENRS and charge efficiency. The former measures the net energy consumption for desalinating unit salt ions from the feedwater, while the latter measures the ratio of net energy consumption for salt desalination (i.e., effective energy consumption) which applies to the whole system (i.e., observed energy consumption). ENRS decreased from 6.69 ± 0.14 μmol J^{-1} at 0.8 V to 3.51 ± 0.17 μmol J^{-1} at 2.0 V, showing a continuous downward trend, whereas the charge efficiency peaked at 90.8 % at 1.8 V and then dropped to 81.0 % at 2.0V. The gradually decreased ENRS indicates that more energy is consumed to remove unit ions from the feedwater at elevated voltage as ions are transported at a higher rate. On the other hand, when a voltage over the critical voltage of water (i.e., 1.23V) is applied, the Faradaic reaction will be accelerated, and part of the energy will be consumed by the water electrolysis process [39]. This will cause inefficient charge loss and energy consumption in an FCDI. This is reflected by the charge efficiency curve in Fig. 1 which reached a peak value of 90.8 % at the voltage of 1.8 V and started to reduce afterward. The effects of advanced water electrolysis eventually surpassed the enhancement caused by EDLs reinforcement, resulting in a reduction in charge efficiency at a voltage higher than 1.8 V. Therefore, although a higher voltage resulted in higher desalination performance, it meanwhile caused an increasing wastage of electric energy. From this perspective, a moderate voltage at approximately 1.8 V is recommended to balance the efficiency of an FCDI between desalination and energy consumption efficiencies.

3.1.2. Effect of AC wt.%

The effect of AC mass content in flow-electrode was investigated within a weight range between 0.5–7.0 wt%. The other operating parameters were set at the initial values as described in section 2.3. The desalination performance and energy efficiency in the lab-scale FCDI under different AC weight ratios are presented in Fig. 2A, while the potential mechanism is illustrated in Fig. 2B.

The SAR_{max}/ASAR of the tested FCDI gradually increased from 0.36 ± 0.01/0.19 ± 0.01 μg cm^{-2} s^{-1} at an AC content of 0.5 wt% and approached a platform at approximately 0.69 ± 0.02/0.23 ± 0.01 μg cm^{-2} s^{-1} as the AC content reached 1.5 wt%. An inflection point of the ASAR curve occurs at the AC content of 2.0 wt%, with the maximum value measured as 0.24 ± 0.01 μg cm^{-2} s^{-1}. Subsequently, as the AC wt.% further increased up to 7.0 wt%, the SAR_{max}/ASAR remained unchanged. The ENRS and charge efficiency showed similar changing trends as the desalination rate, which gradually increased from 4.15 μmol J^{-1} to 76.05 % at AC content of 0.5 wt% to 4.71 μmol J^{-1} and 86.3 % at AC content of 2.0 wt%, respectively, and then it remained constant or even slightly declined with the increased AC contents.

With the AC content rising from 0.5 wt% to 2.0 wt%, the conductivity and total adsorption capacity provided by the flow-electrode material increased accordingly, resulting in increments in both desalination rate and energy efficiency. Simultaneously, as the FCDI system operated in SCC mode, the electrodes were undergoing automatic electrical neutralization, and ion adsorption capacity was regenerated continuously. When the AC content increased greater than 2.0 wt%, the adsorption capacity provided by the electrodes exceeded the demand of a relatively low salinity of feedwater in this study (i.e., 1.0 g L^{-1}). Therefore, both the desalination rate and energy efficiency reached a constant level, and no more increment is expected via further increasing AC content in the flow-electrode. Conversely, further increasing AC content may raise the risk of electrode pathway blockage in the flow channels. Park et al. reported that the salt removal efficiency was enhanced from 8.4 % to 26.5 % as the AC wt.% increased from 10 % to 30 %, while the charge efficiency fluctuated slightly between 74.7 % and 81.3 % [24]. Whereas, in the current study, the effect of increasing AC content in flow-electrode was not as obvious as in the previous report. This was possibly due to the different application scenarios of the two studies: Park et al. focused on the desalination of seawater (feedwater concentration: 30 g L^{-1}); This study paid attention to the desalination of low salinity water (i.e., 1.0 g L^{-1}) affected by seawater intrusion. Compared to an electrolyte concentration of 10.0 g L^{-1}, the increase in AC wt.% showed no significant effect on the conductivity of the flow-electrode. With a low feedwater concentration, low AC wt.% provided sufficient adsorption sites, whereas the excess AC instead consumed energy through Faradaic reactions

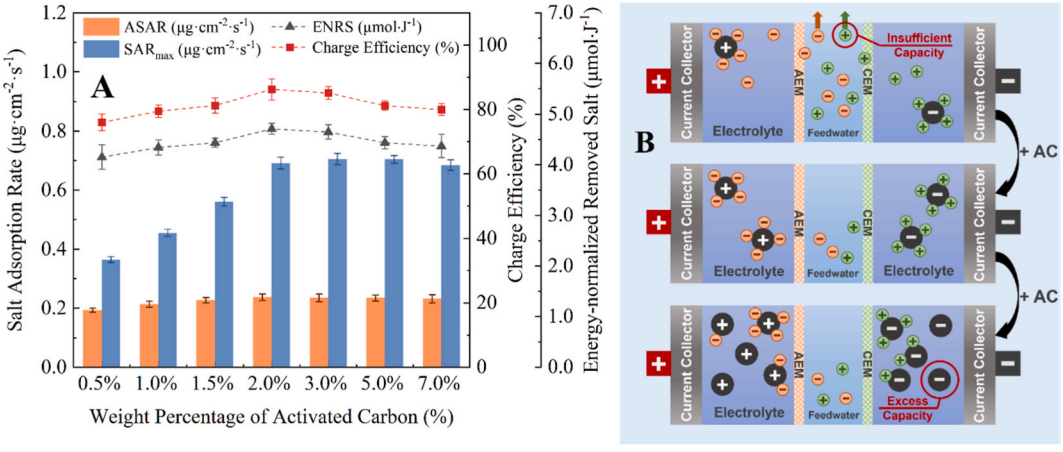

Fig. 2. Desalination performance analysis (A) and mechanism diagram (B) of FCDI system under various AC contents.

and so on [31]. Therefore, in practical operation, the AC wt.% should be determined based on various factors such as feedwater concentration, applied voltage, system operation stability, etc.

3.1.3. Effect of electrolyte concentration

The effect of electrolyte concentration in the flow-electrode of FCDI was investigated with a series of varied NaCl concentrations ranging between 1.0 and 15.0 g L^{-1}, while the other operating parameters were maintained at the initial settings. As shown in Fig. 3A, with the increase of electrolyte concentration, the SAR_{max} and ASAR of FCDI presented a trend of firstly increasing and then decreasing. A peak appeared at an electrolyte concentration of 10.0 g L^{-1}, with the SAR_{max} and ASAR raised from 0.44 ± 0.01/0.16 ± 0.01 μg cm^{-2} s^{-1} at 1.0 g L^{-1} to 0.80 ± 0.01/0.28 ± 0.01 μg cm^{-2} s^{-1} at 10.0 g L^{-1}, respectively. Subsequently, as the electrolyte concentration further increased to 15.0 g L^{-1}, the SAR_{max} and ASAR dropped slightly to 0.66 ± 0.02 and 0.24 ± 0.02 μg cm^{-2} s^{-1}, respectively. Likewise, ENRS dropped from 4.66 μmol J^{-1} at 10.0 g L^{-1} to 4.24 μmol J^{-1} at 15.0 g L^{-1}, and the charge efficiency dropped from 87.7 % to 79.2 % as well.

As illustrated in Fig. 3B, increasing the concentration of electrolyte was able to reduce the resistance of flow-electrodes and hence enhance the mobility of ions from feedwater to electrodes (shown by the light red arrows in Fig. 2B) in FCDI. This explained the initial increment in SAR_{max}/ASAR as electrolyte concentration increased up to 10.0 g L^{-1}. However, as the NaCl concentration increased in the electrolyte, an elevated salt concentration gradient from the flow-electrode to feedwater developed (shown by the dark red arrows in Fig. 2B), which hindered the mass transfer of salt ions in the opposite direction. As a result, when the electrolyte concentration exceeded 10.0 g L^{-1}, the reverse ion migration driven by the enlarged concentration gradient surpassed the positive effect brought by resistance reduction, eventually causing a decrease in desalination efficiency. This also explained why the charge efficiency and ENRS showed a trend of first rising and then falling.

3.1.4. Effect of feedwater flowrate

Fig. 4A shows that with an increasing feedwater flowrate, the SAR_{max}/ASAR was continuously enhanced, from 0.43 ± 0.02/0.18 ± 0.01 μg cm^{-2} s^{-1} at 10 mL min^{-1} to 0.78 ± 0.01/0.26 ± 0.01 μg cm^{-2} s^{-1} at 120 mL min^{-1}. However, this increment became less significant as the feed flowrate increased over 60 mL min^{-1}. Whereas, unlike the desalination rate, ENRS and charge efficiency remained constant at approximately 4.6 ± 0.1 μmol J^{-1} and 85 %, respectively, with varied feed flowrates.

The effect of feedwater flowrates on the desalination rate is possibly associated with the variation of concentration polarization (CP) in FCDI (see Fig. 4B). Due to the higher ion conductivity in the ion exchange membrane than in feedwater, a concentration drop is expected in the liquid film layer from the bulk feed to the membrane surface to overcome the extra electrical energy that needs to be consumed. Increasing feedwater flowrate was able to cause turbulence at the membrane surface and hence, relieved the influence of concentration polarization to a certain extent. Thereby, slight SAR_{max}/ASAR increments were observed at the initial half of their variation curves as functions of feed flowrate. Nevertheless, reducing concentration polarization typically has a limited effect on improving the overall performance of the ion mass transfer [40]. On the other hand, the effect of concentration polarization is not selective to ion species, hence no influence on charge efficiency/ENRS was observed. Previous FCDI studies have also reported on the influence and mitigation of CP. Fang et al. reduced the impact of CP by controlling the concentration factors (CF), while Ma et al. developed ball-milled activated carbon (BAC) with small particle size by grinding AC to alleviate the effect of CP [26,41].

3.1.5. Effect of electrode flowrate

The effect of flow-electrode flowrate was studied with a series of flowrate values designed between 60 and 140 mL min^{-1}. The minimum flowrate of the electrode was set to 60 mL min^{-1} to prevent the precipitation of electrode materials. Fig. 5A revealed that with an increasing flow-electrode flowrate, both the SAR_{max}/ASAR of the FCDI system declined from 0.80 ± 0.02/0.25 ± 0.01 μg

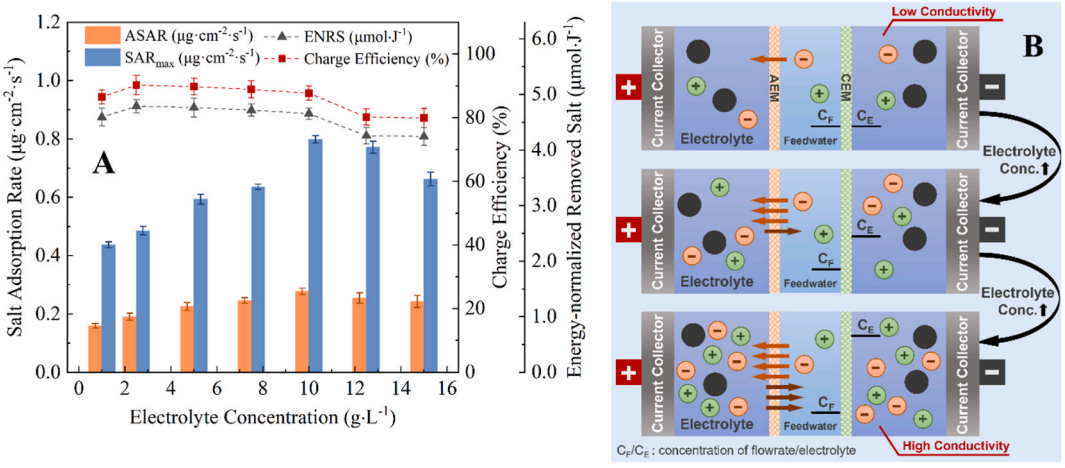

Fig. 3. Desalination performance analysis (A) and mechanism diagram (B) of FCDI system under various electrolyte concentrations.

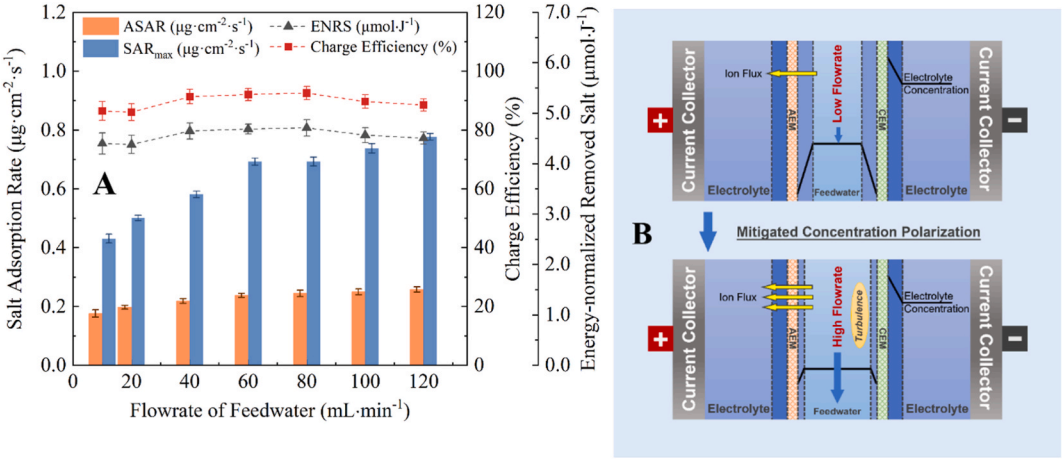

Fig. 4. Desalination performance analysis (A) and mechanism diagram (B) of FCDI system under various feedwater flowrates.

$cm^{-2}\ s^{-1}$ at 60 mL min^{-1} to 0.52 ± 0.02/0.21 ± 0.01 μg $cm^{-2}\ s^{-1}$ at 140 mL min^{-1}. However, charge efficiency and ENRS remained constant at approximately 82 %/4.70 μmol J^{-1}.

As shown in Fig. 5B, intensified fluid shear force in a flow-electrode may cause compression of the thickness of EDLs and hence lower its counter-ion adsorption capacity. In the meanwhile, the adsorbed counter-ions surrounding the EDLs can be easily dissociated due to the increased fluid disturbance. This may explain the observed decrease in SAR_{max}/ASAR in FCDI as the electrode flowrate increased from 60 to 140 mL min^{-1} in this study. Similar to feedwater flowrate, there is no selectivity of ion species due to such fluid mechanics. Hence, no variation in charge efficiency and ENRS was observed.

3.2. *Sensitivity analysis of selected operating parameters*

To identify the key operating parameter affecting the performance of FCDI, a local sensitivity analysis was carried out. Variations ranging up to ±50 % of the initial experimental settings, i.e., feed NaCl concentration of 1.0 g L^{-1}, a voltage of 1.6 V, AC wt.% of 2.0 %, electrolyte concentration of 7.5 g L^{-1}, feedwater flowrate of 60 mL min^{-1}, and electrode flowrate at 100 mL min^{-1} were evaluated, and the percentage changes in ASAR and ENRS are plotted in Fig. 6A and **B**. The larger the absolute value of the gradient, the higher the sensitivity of the FCDI system to the parameter [42].

In practical operation, it is preferable to have the highest possible desalination rate and energy efficiency. The operating voltage presented the most sensitive influence on ASAR and ENRS, both with positive correlations. With a 25 % increment in voltage supply, the ASAR and ENRS raised by approximately 53.1 % and 8.9 %, respectively. Whereas, ASAR and ENRS showed less sensitivity to the variations in electrolyte concentration, AC content, and feedwater flowrate. With a 25 % increment in electrolyte concentration, AC content, and feedwater flowrate, ASAR values are expected to raise by approximately 4.0 %, 0.9 %, and 2.2 %, while negligible variation is expected in ENRS. Different from the other selected parameters, electrode flowrate showed a negative effect with moderate sensitivity to ASAR. With a 25 % reduction of electrode flowrate, a 9.0 % of increment in ASAR is expectable.

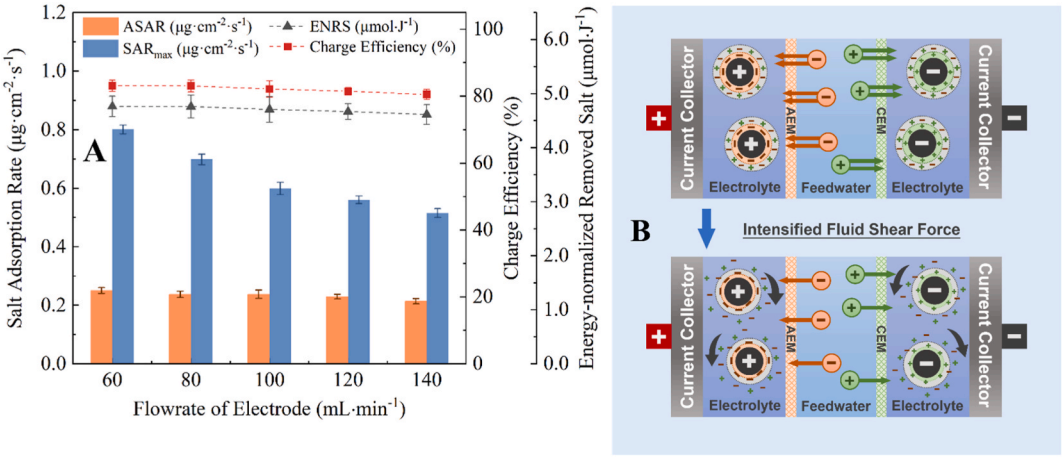

Fig. 5. Desalination performance analysis (A) and mechanism diagram (B) of FCDI system under various electrode flowrates.

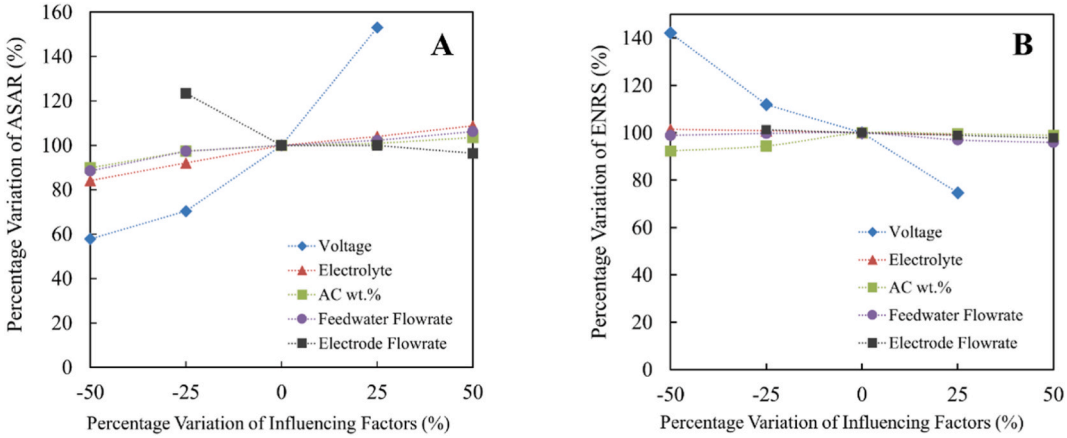

Fig. 6. Sensitivity analysis of selected parameters to ASAR (A) and ENRS (B).

According to the results of sensitivity analysis, the voltage was regarded as the dominant parameter, while electrolyte concentration, electrode flowrate, feedwater flowrate, and AC wt.% were recognized as non-dominant parameters. The increase of voltage directly led to the increment of charge transfer in the system, and the electric field driving force of the ions as well as the thickness of the electric double layers were also enhanced with the voltage [38]. The superposition of these several effects acted directly on the salt ions so that the FCDI system exhibited high sensitivity. AC content was directly linked to the adoption capacity, whose effect may be more significant when treating high-salinity feedwater [15]. Its sensitive effect was not observed due to the relatively low-salinity feedwater tested in the current study. The electrolyte concentration mainly affected the desalination process by changing the electrode conductivity, while its positive effect might be limited by the reverse driving force for ions caused by the cumulation of a salt concentration gradient. As for the variation of the fluid flowrates, they may only affect the degree of concentration polarization and the stability of the adsorption environment to a certain extent, resulting in a limited effect on the system performance as well.

3.3. Long-term operation of FCDI with flow-electrode regeneration

3.3.1. Selection of flow-electrode regeneration method

A preliminary selection of the proper flow-electrode regeneration method was carried out prior to the long-term operation experiment. To screen out an appropriate scheme for electrode material recovery and regeneration, filter membranes with different materials and pore sizes were tested and evaluated systematically. After separating the solid and liquid from the used flow-electrode

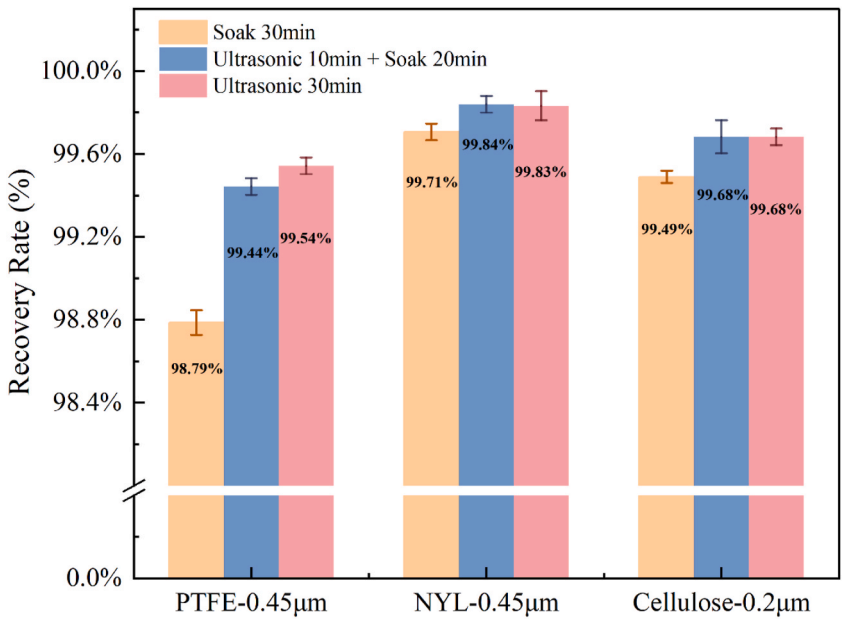

Fig. 7. Electrode material recovery rates using different types of filter membranes and cleaning methods.

solution using a filter membrane and washing away the salt, the filter membranes were further cleaned (soaked or sonicated). A regenerated flow-electrode was prepared using the AC suspension from membrane cleaning and the collected AC solid after filtration. Ensuring that AC was not lost through other pathways, the dry weight of the filter membrane before and after filtration and cleaning was measured, and the recovery rate of the electrode material was calculated using the following equation:

$$Recovery\ rate = \frac{(Initial\ AC\ weight - Filter\ retained\ AC\ weight)}{(Initial\ AC\ weight)} \times 100\% \quad (5)$$

As illustrated in Fig. 7, all three membranes exhibited excellent material retention rates. Among them, NYL-0.45 μm showed the best performance (recovery rate up to 99.84 %), closely followed by Cellulose Acetate-0.2 μm (99.68 %), and PTFE-0.45 μm (99.54 %). Whereas, for the cleaning methods, soaking for 30 min achieved a comparable high recovery rate (>99 %) with low energy consumption. Therefore, by comprehensive consideration of electrode recovery rate and energy consumption, a flow-electrode recovery process composed of filtration using an NYL-0.45 μm membrane and cleaning through soaking for 30 min was selected.

3.3.2. Long-term operation of FCDI

In long-term operation, the single-pass mode of feedwater was employed instead of the circulation mode. According to the standard set by U.S. Environmental Protection Agency (USEPA), the total dissolved solids (TDS) in tap water should not exceed 500 mg L^{-1} (USEPA, 2022). In this lab-scale study, the TDS value reflected the salinity of the synthetic feedwater (i.e., NaCl solution). To ensure that the HRT of feedwater was sufficient to achieve this effluent requirement, a feedwater flowrate of 2 mL min^{-1} was adopted.

Fig. 8 profiles the variation of effluent NaCl concentration, desalination efficiency, and ENRS of the FCDI system during the long-term operation. In each operating cycle, the desalination efficiency presented a three-phase variation, namely the start-up phase - steady phase – declining phase. Taking the first cycle as an example, a sharp effluent concentration dropped from 1000 mg L^{-1} to about 500 mg L^{-1} and desalination efficiency rose from 0 to 50.94 % in the start-up phase (i.e., initial 1.0 h). This was attributed to the insufficient residence time for saltwater remaining in the feed channel at the beginning of the operation, so the effluent concentration dropped rapidly. The duration of the start-up phase depended on the designed feedwater flowrate and typically lasted for a short period. In the steady phase (i.e., 1.0–19.0 h), a relatively high desalination efficiency (50.94–67.53 %) and low effluent salt concentration (486.7–316.4 mg L^{-1}) were maintained with the desalination performance continually going upwards. With the progress of desalination, increasing salt ions accumulated in the flow-electrode causes a reduction in the cell resistance and thereby further advancing its desalination efficiency. Whereas, along with such ion accumulation, the salt concentration gradient across the ion exchange membranes was gradually climbing, which created an ion-driving force in the direction opposite to the electric field. This gradually offset the increased desalination due to the lowered resistance and eventually outweighed the above enhancement, resulting in the desalination efficiency to start declining over time (i.e., decline phase). The desalination decline occurred gently and lasted for approximately 30 h, which allowed a relatively stable operation of FCDI up to 50 h to ensure a minimum desalination efficiency of 50 %. Unlike the desalination curve, which rose first and then fell, ENRS showed a continuous downward trend after the system stabilized. The increase in the overall conductivity of the system did not affect the ion transfer process, and the decrease in ENRS may be attributed to the increasing concentration gradient between the flow-electrode and the feedwater.

During an approximately 170-h operation, the lab-scale FCDI indicated a good potential of the system for long-term desalination with a stable performance. Using a 2 wt% AC electrode, the FCDI was able to sustain a desalination efficiency above 50 % for 1.0 g L^{-1} salt water for 50 h and produce 6.0 L effluent per repeatable operation cycle. The peak desalination efficiency in each cycle was successively measured as 67.5 %, 66.4 %, and 64.7 %, respectively. Previous studies have reported substantial performance depletion of carbon-based electrode materials that occurred in FCDI due to the impact of the Faradaic reaction and carbon oxidation, which could cause a collapse of pore structure, reduction of surface area, and increase of resistance [31,44]. Zhang et al. reported an approximately 10 % specific surface area loss on the carbon-based flow-electrode (9 % activated carbon + 1 % carbon black) which dropped from 1100 $cm^2\ g^{-1}$ to 991 $cm^2\ g^{-1}$ in a 14-day operation [43]. Conversely, the current study did not observe a statistically significant decrease in the performance of the flow-electrode, which may indicate that the carbon material properties were not significantly affected during 170 h of operation. Nonetheless, to clarify and improve the regeneration rate and performance maintenance of carbon materials, it is imperative to conduct longer FCDI operations with more repetition cycles in the future.

4. Conclusions

This study carried out a systematic optimization of the key operating parameters in a lab-scale FCDI system and interpreted the potential influencing mechanisms of selected parameters on the performance of FCDI. The optimal combination of the parameters for low-concentration brine desalination was determined as the voltage of 1.8V, the electrolyte concentration of 10 g L^{-1}, the electrode material content of 2 wt%, the feedwater flowrate of 80 mL min^{-1}, and the electrode flowrate of 60 mL min^{-1}. The above parameters affected the performance of FCDI mainly by influencing the charge transfer, adsorption capacity, concentration polarization, and the electrical double layers. The results of sensitivity analysis indicated that the dominant parameter was operating voltage, which caused a 53.1 % rise in the desalination rate with a 25 % voltage increment. Whereas, the other four parameters showed less influence on the performance of FCDIs. Microfiltration using a 0.45 membrane filter associated with soak cleaning provided 99.8 % recovery of the AC electrode and was selected for flow-electrode regeneration during long-term operation. A long-term operation of approximately 170 h (containing three cycles) was demonstrated with the optimized operating conditions and selected electrode regeneration method. The results showed that the lab-scale FCDI system kept the desalination efficiency of 1 g L^{-1} saltwater above 50 % continuously for 50–60

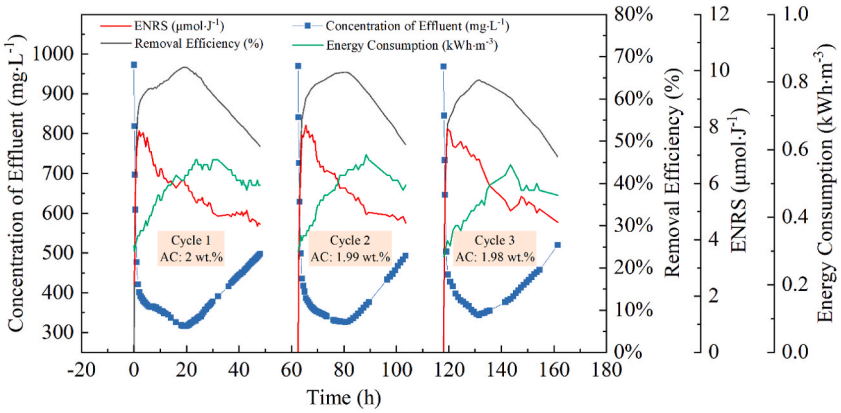

Fig. 8. Variation of effluent concentration, desalination efficiency, and ENRS of FCDI system during long-term operation.

h, which produced 6.0 L effluent per cycle with an average energy consumption of 0.45 kWh m^{-3}. Furthermore, the loss of electrode material was merely approximately 1 % after each cycle. The high recovery of electrode materials and the satisfactory long-term operational stability of the FCDI system reported in this study provide a reference for the practical application of FCDI.

Data availability statement

Data will be made available on request.

CRediT authorship contribution statement

Wanni Zhang: Writing – original draft. **Wenchao Xue:** Writing – review & editing, Supervision, Resources, Methodology, Funding acquisition, Conceptualization. **Chunpeng Zhang:** Writing – review & editing, Supervision, Funding acquisition. **Kang Xiao:** Writing – review & editing.

Declaration of competing interest

The authors declare that they have no known competing financial interests or personal relationships that could have appeared to influence the work reported in this paper.

Acknowledgment

This work was supported by the National Research Council of Thailand (Grant No. N10E650034) and the National Natural Science Foundation of China (Grant No. 42107483).

Appendix A. Supplementary data

Supplementary data to this article can be found online at https://doi.org/10.1016/j.heliyon.2024.e24940.

References

[1] K. Elsaid, M. Kamil, E.T. Sayed, M.A. Abdelkareem, T. Wilberforce, A. Olabi, Environmental impact of desalination technologies: a review, Sci. Total Environ. 748 (2020) 141528, https://doi.org/10.1016/J.SCITOTENV.2020.141528.
[2] Y.J. Lim, K. Goh, M. Kurihara, R. Wang, Seawater desalination by reverse osmosis: current development and future challenges in membrane fabrication – a review, J. Membr. Sci. 629 (2021) 119292, https://doi.org/10.1016/J.MEMSCI.2021.119292.
[3] S. Lin, H. Zhao, L. Zhu, T. He, S. Chen, C. Gao, L. Zhang, Seawater desalination technology and engineering in China: a review, Desalination 498 (2021) 114728, https://doi.org/10.1016/J.DESAL.2020.114728.
[4] D. Zhou, L. Zhu, Y. Fu, M. Zhu, L. Xue, Development of lower cost seawater desalination processes using nanofiltration technologies — a review, Desalination 376 (2015) 109–116, https://doi.org/10.1016/J.DESAL.2015.08.020.
[5] T. Feng, Q. Liu, C. Yang, G. Li, J. Liu, Membrane capacitive deionization (MCDI) for removal of chromium complexes with AC@SiO2-NH2 electrode, J. Environ. Chem. Eng. 10 (2022) 108363, https://doi.org/10.1016/J.JECE.2022.108363.
[6] J.J. Lado, V. Cartolano, E. García-Quismondo, G. García, I. Almonacid, V. Senatore, V. Naddeo, J. Palma, M.A. Anderson, Performance analysis of a capacitive deionization stack for brackish water desalination, Desalination 501 (2021) 114912, https://doi.org/10.1016/J.DESAL.2020.114912.
[7] S.Y. Pan, A.Z. Haddad, A. Kumar, S.W. Wang, Brackish water desalination using reverse osmosis and capacitive deionization at the water-energy nexus, Water Res. 183 (2020) 116064, https://doi.org/10.1016/J.WATRES.2020.116064.

[8] S. Il Jeon, H.R. Park, J.G. Yeo, S. Yang, C.H. Cho, M.H. Han, D.K. Kim, Desalination via a new membrane capacitive deionization process utilizing flow-electrodes, Energy Environ. Sci. 6 (2013) 1471–1475, https://doi.org/10.1039/c3ee24443a.

[9] C. Zhang, J. Ma, L. Wu, J. Sun, L. Wang, T. Li, T. David Waite, Flow electrode capacitive deionization (FCDI): recent developments, environmental applications, and future perspectives, Environ. Sci. Technol. 55 (2021) 4243–4267, https://doi.org/10.1021/acs.est.0c06552.

[10] J. Ma, C. Zhai, F. Yu, Review of flow electrode capacitive deionization technology: research progress and future challenges, Desalination 564 (2023) 116701, https://doi.org/10.1016/j.desal.2023.116701.

[11] Y. Gendel, A.K.E. Rommerskirchen, O. David, M. Wessling, Batch mode and continuous desalination of water using flowing carbon deionization (FCDI) technology, Electrochem. Commun. 46 (2014) 152–156, https://doi.org/10.1016/j.elecom.2014.06.004.

[12] K.B. Hatzell, M.C. Hatzell, K.M. Cook, M. Boota, G.M. Housel, A. McBride, E. Caglan Kumbur, Y. Gogotsi, Effect of oxidation of carbon material on suspension electrodes for flow electrode capacitive deionization, Environ. Sci. Technol. 49 (2015) 3040–3047, https://doi.org/10.1021/es5055989.

[13] P. Srimuk, X. Su, J. Yoon, D. Aurbach, V. Presser, Charge-transfer materials for electrochemical water desalination, ion separation and the recovery of elements, Nat. Rev. Mater. 5 (2020) 517–538, https://doi.org/10.1038/s41578-020-0193-1, 2020 5:7.

[14] Y. Cho, C.Y. Yoo, S.W. Lee, H. Yoon, K.S. Lee, S.C. Yang, D.K. Kim, Flow-electrode capacitive deionization with highly enhanced salt removal performance utilizing high-aspect ratio functionalized carbon nanotubes, Water Res. 151 (2019) 252–259, https://doi.org/10.1016/j.watres.2018.11.080.

[15] P. Liang, X. Sun, Y. Bian, H. Zhang, X. Yang, Y. Jiang, P. Liu, X. Huang, Optimized desalination performance of high voltage flow-electrode capacitive deionization by adding carbon black in flow-electrode, Desalination 420 (2017) 63–69, https://doi.org/10.1016/J.DESAL.2017.05.023.

[16] W. Zhang, W. Xue, K. Xiao, C. Visvanathan, J. Tang, L. Li, Selection and optimization of carbon-based electrode materials for flow-electrode capacitive deionization, Sep. Purif. Technol. 315 (2023) 123649, https://doi.org/10.1016/j.seppur.2023.123649.

[17] P. Nativ, Y. Badash, Y. Gendel, New insights into the mechanism of flow-electrode capacitive deionization, Electrochem. Commun. 76 (2017) 24–28, https://doi.org/10.1016/J.ELECOM.2017.01.008.

[18] A. Rommerskirchen, B. Ohs, K.A. Hepp, R. Femmer, M. Wessling, Modeling continuous flow-electrode capacitive deionization processes with ion-exchange membranes, J. Membr. Sci. 546 (2018) 188–196, https://doi.org/10.1016/J.MEMSCI.2017.10.026.

[19] Y. Cho, K.S. Lee, S.C. Yang, J. Choi, H.R. Park, D.K. Kim, A novel three-dimensional desalination system utilizing honeycomb-shaped lattice structures for flow-electrode capacitive deionization, Energy Environ. Sci. 10 (2017) 1746–1750, https://doi.org/10.1039/C7EE00698E.

[20] J.J. Ma, J.J. Ma, C. Zhang, J. Song, W. Dong, T.D. Waite, Flow-electrode capacitive deionization (FCDI) scale-up using a membrane stack configuration, Water Res. 168 (2020) 115186, https://doi.org/10.1016/J.WATRES.2019.115186.

[21] W. Xing, J. Liang, W. Tang, D. He, M. Yan, X. Wang, Y. Luo, N. Tang, M. Huang, Versatile applications of capacitive deionization (CDI)-based technologies, Desalination 482 (2020) 114390, https://doi.org/10.1016/J.DESAL.2020.114390.

[22] J.E. Dykstra, S. Porada, A. van der Wal, P.M. Biesheuvel, Energy consumption in capacitive deionization – constant current versus constant voltage operation, Water Res. 143 (2018) 367–375, https://doi.org/10.1016/J.WATRES.2018.06.034.

[23] J. Ma, C. Zhang, F. Yang, X. Zhang, M.E. Suss, X. Huang, P. Liang, Carbon black flow electrode enhanced electrochemical desalination using single-cycle operation, Environ. Sci. Technol. 54 (2019) 1177–1185, https://doi.org/10.1021/acs.est.9b04823.

[24] H.R. Park, J. Choi, S. Yang, S.J. Kwak, S. Il Jeon, M.H. Han, D.K. Kim, Surface-modified spherical activated carbon for high carbon loading and its desalting performance in flow-electrode capacitive deionization, RSC Adv. 6 (2016) 69720–69727, https://doi.org/10.1039/c6ra02480g.

[25] T. Wen, G.S. Solt, D.W. Gao, Electrical resistance and coulomb efficiency of electrodialysis (ED) apparatus in polarization, J. Membr. Sci. 114 (1996) 255–262, https://doi.org/10.1016/0376-7388(96)00005-1.

[26] D. Henderson, D. Boda, Insights from theory and simulation on the electrical double layer, Phys. Chem. Chem. Phys. 11 (2009) 3822–3830, https://doi.org/10.1039/B815946G.

[27] W.H. Duan, Q. Wang, F. Collins, Dispersion of carbon nanotubes with SDS surfactants: a study from a binding energy perspective, Chem. Sci. 2 (2011) 1407–1413, https://doi.org/10.1039/c0sc00616e.

[28] Y. Cai, X. Zhao, Y. Wang, D. Ma, S. Xu, Enhanced desalination performance utilizing sulfonated carbon nanotube in the flow-electrode capacitive deionization process, Sep. Purif. Technol. 237 (2020) 116381, https://doi.org/10.1016/J.SEPPUR.2019.116381.

[29] M. Sillanpää, M. Shestakova, Emerging and combined electrochemical methods, Electrochem. Water Treat. Methods Fundam. Methods Full Scale Appl. (2017) 131–225, https://doi.org/10.1016/B978-0-12-811462-9.00003-7.

[30] C. Zhang, D. He, J. Ma, W. Tang, T.D. Waite, Faradaic reactions in capacitive deionization (CDI) - problems and possibilities: a review, Water Res. 128 (2018) 314–330, https://doi.org/10.1016/J.WATRES.2017.10.024.

[31] Z. Ghazali, M.A.A. Majid, T.C. Chi, Engineering economic analysis for feed gas cooler (cold box): a case of a gas processing complex in Malaysia, MATEC Web of Conferences 13 (2014) 05009, https://doi.org/10.1051/matecconf/20141305009.

[32] E. Avraham, M. Noked, Y. Bouhadana, A. Soffer, D. Aurbach, Limitations of charge efficiency in capacitive deionization processes III: the behavior of surface oxidized activated carbon electrodes, Electrochim. Acta 56 (2010) 441–447, https://doi.org/10.1016/J.ELECTACTA.2010.08.056.

[33] C. He, J. Ma, C. Zhang, J. Song, T. David Waite, Short-circuited closed-cycle operation of flow-electrode CDI for brackish water softening, Environ. Sci. Technol. 52 (2018) 9350–9360, https://doi.org/10.1021/acs.est.8b02807.

[34] K. Tang, S. Yiacoumi, Y. Li, C. Tsouris, Enhanced water desalination by increasing the electroconductivity of carbon powders for high-performance flow-electrode capacitive deionization, ACS Sustain. Chem. Eng. 7 (2018) 1085–1094, https://doi.org/10.1021/acssuschemeng.8b04746.

[35] F. Yu, Z. Yang, Y. Cheng, S. Xing, Y. Wang, J. Ma, A comprehensive review on flow-electrode capacitive deionization: design, active material and environmental application, Sep. Purif. Technol. 281 (2022) 119870, https://doi.org/10.1016/j.seppur.2021.119870.

[36] A. Campione, L. Gurreri, M. Ciofalo, G. Micale, A. Tamburini, A. Cipollina, Electrodialysis for water desalination: a critical assessment of recent developments on process fundamentals, models and applications, Desalination 434 (2018) 121–160, https://doi.org/10.1016/j.desal.2017.12.044.

[37] J. Chang, F. Duan, H. Cao, K. Tang, C. Su, Y. Li, Superiority of a novel flow-electrode capacitive deionization (FCDI) based on a battery material at high applied voltage, Desalination 468 (2019) 114080, https://doi.org/10.1016/J.DESAL.2019.114080.

[38] H. Li, L. Zou, Ion-exchange membrane capacitive deionization: a new strategy for brackish water desalination, Desalination 275 (2011) 62–66, https://doi.org/10.1016/J.DESAL.2011.02.027.

[39] S. Ilias, R. Govind, A study on concentration polarization in ultrafiltration, Separ. Sci. Technol. 28 (1993) 361–381. https://api.semanticscholar.org/CorpusID:96758599.

[40] K. Fang, F. Peng, E. San, K. Wang, The impact of concentration in electrolyte on ammonia removal in flow-electrode capacitive deionization system, Sep. Purif. Technol. 255 (2021) 117337, https://doi.org/10.1016/j.seppur.2020.117337.

[41] J. Ma, G. Shen, R. Zhang, J. Niu, J. Zhang, X. Wang, J. Liu, X. Li, C. Liu, Small particle size activated carbon enhanced flow electrode capacitive deionization desalination performances by reducing the interfacial concentration difference, Electrochim. Acta 431 (2022) 140971, https://doi.org/10.1016/j.electacta.2022.140971.

[42] M. Poirier-Pocovi, B.N. Bailey, Sensitivity analysis of four crop water stress indices to ambient environmental conditions and stomatal conductance, Sci. Hortic. 259 (2020) 108825, https://doi.org/10.1016/J.SCIENTA.2019.108825.

[43] C. Zhang, L. Wu, J. Ma, M. Wang, J. Sun, T.D. Waite, Evaluation of long-term performance of a continuously operated flow-electrode CDI system for salt removal from brackish waters, Water Res. 173 (2020) 115580, https://doi.org/10.1016/J.WATRES.2020.115580.

[44] J.H. Choi, Determination of the electrode potential causing Faradaic reactions in membrane capacitive deionization, Desalination 347 (2014) 224–229, https://doi.org/10.1016/J.DESAL.2014.06.004.